Characterizing the Secondary Structure and Identifying Functionally Essential Nucleotides of pH6DZ1, a Fluorescence-Signaling and RNA-Cleaving Deoxyribozyme†

Yutu Shen, John D. Brennan, and Yingfu Li*

Department of Biochemistry and Biomedical Sciences and Department of Chemistry, McMaster University, 1200 Main Street West, Hamilton, Ontario L8N 3Z5, Canada

Received April 22, 2005; Revised Manuscript Received July 5, 2005

ABSTRACT: pH6DZ1 is a synthetic deoxyribozyme that is able to couple catalysis with fluorescence signal generation. This deoxyribozyme has the ability to cleave itself at a lone ribonucleotide that is present between a pair of deoxyribothymidines, one modified with a fluorophore (fluorescein) and the other with a quencher (DABCYL). Herein, we report on the sequence truncation and secondary structure characterization of pH6DZ1 as well as the identification of functionally important nucleotides within this deoxyribozyme. Our data indicate that pH6DZ1 has a four-way, junction-like secondary structure comprised of four short duplexes, three hairpin loops, and three interhelical unpaired elements. Ten nucleotides, all located in two separate single-stranded regions, were identified as functionally indispensable nucleotides (complete loss of the catalytic function was obtained upon mutation). Nine nucleotides, most of which are also distributed in three single-stranded DNA elements, were identified as functionally vital nucleotides (at least a 1000-fold activity reduction was obtained upon mutation). Our study has shown that pH6DZ1 has a secondary structure that is more complex than those reported for other RNA-cleaving deoxyribozymes. The identification of functionally important nucleotides lays the foundation for future mechanistic studies on this DNAzyme. The elucidation of the secondary structure of pH6DZ1 should facilitate the future exploration of this unique DNAzyme for the development of DNAzyme-based biosensors.

Deoxyribozymes, also known as DNAzymes or DNA enzymes, are synthetic DNA oligonucleotides with the ability to catalyze diverse chemical reactions (*1*−*3*). We recently performed an in vitro selection study from which several fluorescence-signaling, RNA-cleaving deoxyribozymes were isolated (*4*). These signaling deoxyribozymes were derived on the basis of their ability to cleave an attached RNA/DNA chimeric substrate in which a lone RNA linkage was flanked immediately by two deoxyribothymidine residues containing a fluorophore (fluorescein) and a quencher (DABCYL),[1] respectively. The physical proximity of the fluorophore and the quencher results in efficient fluorescence quenching prior to the catalytic cleavage of the lone ribonucleotide. Upon RNA cleavage, the fluorophore moves away from the quencher, leading to an intense fluorescence signal. Because of the uniquely linked catalysis−signaling capability, these special RNA-cleaving deoxyribozymes offer an excellent opportunity for designing DNAzyme based biosensors (*5*, *6*).

The most desirable biosensing application for these unique DNAzymes is the design of allosteric signaling deoxyribozymes for the real-time detection of chemical and biological ligands (*5*). However, engineering such allosteric signaling deoxyribozymes requires detailed knowledge of the secondary structures of these single-stranded DNA molecules. Therefore, elucidating their secondary structures is imperative to realize their full biosensing potential. Moreover, the elucidation of their secondary structures will allow us to determine whether these RNA-cleaving DNA catalysts share secondary-structural features that are similar to those exhibited by several known deoxyribozymes that cleave unmodified RNA substrates (*7*−*11*). This in turn will address the question of whether single-stranded DNA can use diverse structures to perform a similar catalytic task.

In this report, we sought to examine the secondary-structural properties of a previously isolated signaling DNAzyme denoted "pH6DZ1" (*4*). This autocatalytic DNA exhibits a fairly robust catalytic activity (k_{obs} of ∼0.2 min^{-1}), a large signaling magnitude (∼10-fold fluorescence enhancement), a unique metal-ion dependence (requiring both Mn^{2+} and Ni^{2+} for optimal activity), and an intriguing pH profile (a bell curve with an optimal pH of 6) (*4*). These phenotypic properties hint at the possibility that pH6DZ1 may have a unique secondary structure that is worth probing. In this

† This work was supported by research grants from MDS-Sciex, the Natural Sciences and Engineering Research Council of Canada, the Canadian Institutes for Health Research, the Canada Foundation for Innovation, and the Ontario Innovation Trust. Y.L. is a Canada Research Chair in Nucleic Acids Biochemistry. J.D.B. holds the Canada Research Chair in Bioanalytical Chemistry.

* To whom correspondence should be addressed. E-mail, liying@mcmaster.ca; tel, (905) 525-9140 ext. 22462; fax, (905) 522-9033.

[1] Abbreviations: ATP, adenosine 5′-triphosphate; DABCYL, 4-(4-dimethylaminophenylazo)benzoic acid; DMS, dimethyl sulfate; DTT, dithiothreitol; EDTA, ethylenediamine tetraacetic acid; HEPES, *N*-2-hydroxyethylpiperazine-*N*′-2-ethanesulfonic acid; PAGE, polyacrylamide gel electrophoresis; T4 PNK, T4 polynucleotide kinase; TOM, triisopropylsilyloxymethyl.

10.1021/bi050746f CCC: $30.25
Published on Web 08/18/2005

study, we carried out comprehensive sequence truncations and nucleotide alterations to achieve the following three goals: (1) minimizing the size of pH6DZ1, (2) establishing its secondary structure, and (3) categorizing its composite nucleotides according to their functional importance. While the first two objectives were explored to obtain crucial information for potential biosensor engineering, the third goal was critical to laying the foundation for future mechanistic studies on this DNAzyme.

MATERIALS AND METHODS

Oligonucleotides and Other Materials. Standard and modified DNAs were prepared by automated chemical synthesis (HHMI-Keck Biotechnology Resource Laboratory, Yale University; Central Facility, McMaster University) using standard phosphoramidite chemistry. DNA oligonucleotides were purified by 10% preparative denaturing (8 M urea) polyacrylamide gel electrophoresis (PAGE). The 2′-hydroxyl protecting triisopropylsilyloxymethyl (TOM) group of the RNA linkage was removed using a previously reported method (*5*). Nucleoside 5′-triphosphates and [γ-^{32}P]ATP were purchased from Amersham Pharmacia. T4 DNA ligase and T4 polynucleotide kinase (T4 PNK) were purchased from MBI Fermentas. All other chemical reagents were purchased from Sigma and used without further purification.

The reaction buffer used for all catalytic assays contained a final concentration of 800 mM Na^+, 8 mM Mn^{2+}, 2 mM Ni^{2+}, and 50 mM HEPES, pH 6.0 (produced from a 2× stock). The stop solution contained 40 mM EDTA, 8 M urea, 90 mM Tris, 90 mM boric acid, 10% sucrose (w/v), 0.025% xylene cyanol, and 0.025% bromophenol blue. DNA phosphorylation reactions were performed in a 50 mM Tris-HCl (pH 7.6, 25 °C), 10 mM $MgCl_2$, 5 mM DTT, 0.1 mM spermidine, and 0.1 mM EDTA solution containing 0.1 units/μL of PNK. DNA ligation reactions were carried out in a solution containing 40 mM Tris-HCl (pH 7.8, 25 °C), 10 mM $MgCl_2$, 10 mM DTT, 0.5 mM ATP, and 0.05 units/μL of T4 DNA ligase.

Deoxyribozyme Activity Assays. All the cis-acting pH6DZ1 variants required for the sequence truncation and nucleotide mutation studies were constructed in the following way: a relevant catalytic domain was 5′-labeled with 10 μCi of [γ-^{32}P]ATP using PNK. After a 60-min incubation, the 5′-phosphorylated catalyst was ligated to a relevant substrate sequence in the presence of an appropriate DNA template using T4 DNA ligase for 1 h at room temperature. The ligated DNA construct was purified by 10% denaturing PAGE and isolated by the crush and soak method (*12*), followed by ethanol precipitation (repeated twice). The resulting precipitate was redissolved in deionized water. After heating at 90 °C for 1 min and cooling to room temperature for 5 min, the RNA cleavage reaction was initiated by adding the required reaction buffer (used as a 2× stock). The final DNA concentration was set at ~0.1 μM. At 0.1, 1, 10, 100, and 1000 min, an aliquot of the solution was quenched with the stop solution, followed by freezing at −20 °C. Cleavage products were separated by 10% denaturing PAGE, and product yields were determined by quantitating product bands using a PhosphoImager and ImageQuant software (Molecular Dynamics). The catalytic ability of the DNAzyme was scored using the following scheme: any deoxyribozyme construct exhibiting ≥10% cleavage in 1 min was given the highest score at "+++++"; mutant deoxyribozymes with ≥10% cleavage in 10, 100, and 1000 min were scored "++++", "+++", and "++", respectively; those with less than 10% cleavage in 1000 min were given a "+"; molecules that produced no cleavage bands after incubation for 1000 min were denoted by a "-". At least two independent assays were conducted for each deoxyribozyme construct to ensure that the scoring was accurate.

DMS Methylation Interference Assays. The method to be described below was adapted from a previously published protocol (*13*). The relevant deoxyribozyme construct was made as follows: 500 pmol of donor DNA (a relevant catalyst domain) was phosphorylated with a trace amount of [γ-^{32}P]ATP using PNK (0.1 units/μL, final concentration) for 20 min at 37 °C, and was then supplemented with nonradioactive ATP to a final concentration of 1 mM and incubated at 37 °C for another 20 min to ensure complete phosphorylation. PNK was inactivated by heating the reaction mixture at 90 °C for 5 min. The phosphorylation reaction mixture was directly added to a ligation reaction mixture containing 600 pmol DNA template and 550 pmol acceptor DNA (a required substrate domain). The ligation reaction was initiated by adding T4 DNA ligase and allowed to proceed at room temperature for 5 h. After ethanol precipitation, the ligated DNA was isolated by 10% denaturing PAGE.

One hundred picomoles of the above DNA construct in water was heated at 90 °C for 30 s and cooled to room temperature for 5 min. The self-cleavage reaction was initiated by adding the 2× reaction buffer, and the resultant mixture was incubated for 30 min at room temperature. The reaction was quenched by adding 30 mM EDTA (final concentration). The DNA recovered by ethanol precipitation was resuspended in 500 μL of water, heated at 90 °C for 1 min, and quickly cooled to room temperature. An equal volume of 0.4% (v/v) DMS (dimethyl sulfate, freshly made) was added, and the mixture was incubated at room temperature for 40 min. Methylated DNA was recovered by ethanol precipitation, followed by two washes with cold 70% ethanol. This sample was labeled as the "control".

Another 100 pmol DNAzyme construct was also methylated with DMS using the protocol described above. This methylated DNA was then allowed to self-cleave in the reaction buffer for 30 min using a similar procedure to that described for the unmethylated DNA. After the self-cleavage reaction, the DNA was recovered by ethanol precipitation, followed by two washes with 70% ethanol. This sample was labeled as the "test".

Both the control and test DNA samples were 5′-labeled with 20 μCi [γ-^{32}P]ATP using PNK at 37 °C for 20 min. After ethanol precipitation, the 5′-labeled 3′-cleavage fragment (containing the catalytic domain) was purified by 10% denaturing PAGE. These modified oligonucleotides were dissolved in 10% (v/v) piperidine (100 μL, freshly made) and heated at 90 °C for 30 min. The resultant cleaved products were dried under vacuum. The dried pellet was resuspended in 25 μL deionized water and evaporated to dryness under vacuum (twice). The cleaved products were then analyzed by denaturing 10% PAGE.

Densitometry on bands from both the test and control lanes was performed to score the degree of methylation interference observed. The difference in background-corrected band

intensity between equivalent cleavage fragments from each lane was normalized using the difference observed in a pair of cleavage fragments originating from a guanine located in the confirmed catalytically unimportant stem-loop region of the deoxyribozyme construct. The ratio of intensities for each pair of bands (R) was determined by dividing the corrected band intensity in lane T (sample lane) by the corrected band intensity from lane C (control lane). These ratios were then normalized on a scale from 0 to 100, where 0 indicates the least interference and 100 the most, using the following equation:

$$R_{\text{normalized}} = [(R - R_0)/(R_{100} - R_0)] \times 100$$

Metal Specificity. The metal-ion specificity of pH6DZ1 and EC56 (a minimized version of pH6DZ1) was determined by monitoring the ability of each DNA enzyme (containing an internal ^{32}P-labeled phosphodiester linkage, see main text) to undergo self-cleavage, as demonstrated by the presence of a cleavage product on a 10% denaturing PAGE gel. Specific metal-ion concentrations that were tested are listed in the caption to Figure 10. Each *cis* DNAzyme construct was allowed to cleave for 10 min prior to the stopping of the reaction and analyzing the reaction mixture by PAGE. Both a phosphorimage (taken on a Storm 820 Phosphorimager, Molecular Dynamics) and a fluorimage (taken on a Typhoon 9200, Molecular Dynamics) were obtained following gel electrophoresis to examine for radioactivity and fluorescence in the DNA bands.

pH Dependence. Both pH6DZ1 and EC56 (containing an internal ^{32}P-labeled phosphodiester linkage after the cleavage site) were allowed to undergo the RNA cleavage reaction for 10 min under the optimal metal-ion conditions at various pH values, as shown in Figure 11. The reaction was then stopped, analyzed by 10% denaturing PAGE, and scanned for both radioactivity and fluorescence in the DNA bands.

RESULTS

Scoring Catalytic Activity of Mutant Deoxyribozyme Constructs. The primary sequence of pH6DZ1, shown in Figure 1A, is divided into two domains labeled "substrate" (italicized letters) and "catalyst" (normal letters) to reflect the fact that this deoxyribozyme was originally isolated from a library of 100-nt single-stranded DNA molecules (ssDNAs) to which the 23-nt substrate was ligated. For convenience, we numbered the nucleotides in the substrate domain from −1 to −23 in the 3′−5′ direction and those in the catalytic domain from 1 to 100 in the 5′−3′ direction. The specific numeral given to each nucleotide remains unchanged throughout this report, even though many mutant deoxyribozyme constructs had one or more internal nucleotides removed. We note that the substrate domain contains three special nucleotides: the fluorescein-containing deoxyribothymidine (**F**; Fluorescein-dT) at the −10th position, the DABCYL-containing deoxyribothymidine (**Q**; DABCYL-dT; DABCYL: 4-(4-dimethylaminophenylazo)benzoic acid) at the −8th nucleotide, and an adenosine ribonucleotide (**A**) located between **F** and **Q**. The ribonucleotide acts as the lone RNA cleavage site, while **F** and **Q** provide the required situation for fluorescence signaling upon catalysis, allowing for future biosensor engineering.

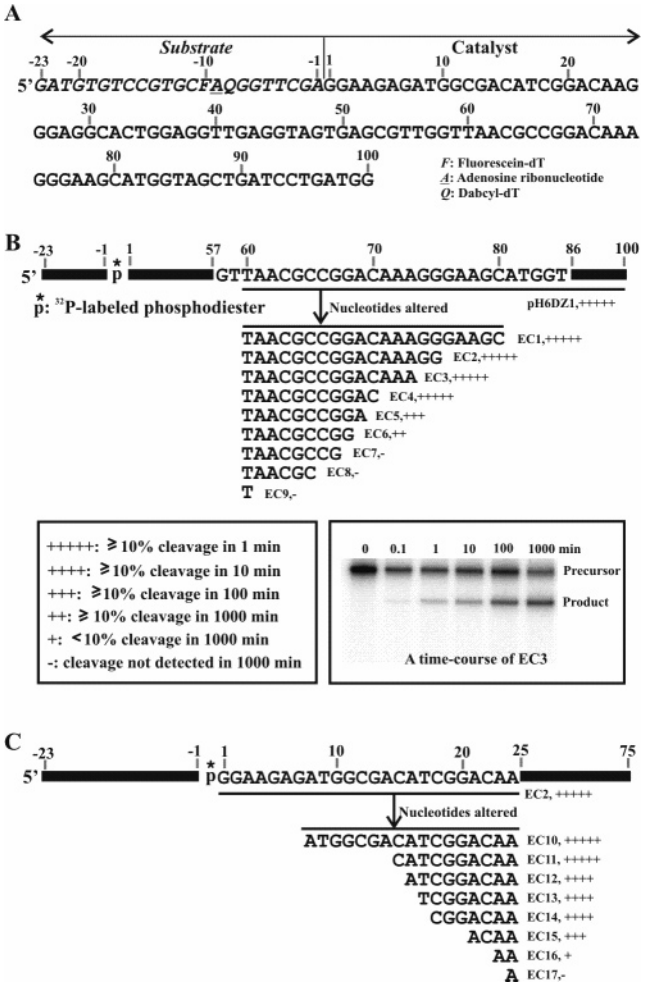

FIGURE 1: The nucleotide sequence of pH6DZ1 and the activity of various truncated deoxyribozymes. (A) The primary sequence of pH6DZ1. The self-cleaving deoxyribozyme is divided into the "substrate" domain (italicized letters; numbered −1 to −23 in the 3′−5′ direction) and the "catalyst" domain (normal letters only; numbered 1 to 100 in the 5′−3′ direction). (B) Results of truncating nucleotides from the 3′ end of the catalytic domain. The reference sequence is pH6DZ1. (C) Results of truncating nucleotides from the 5′ end of the catalytic domain. The reference sequence is EC2. Underlined nucleotides are the region under investigation, with the vertical arrow pointing to all mutated sequences. The identities of the nucleotides represented by black bars are omitted for clarity. The name of each mutant deoxyribozyme is listed next to its altered sequence. The activity of each construct in this figure (as well as in all remaining figures) is scored using the activity map shown as the left inset in panel B. The right inset in panel B is a representative PAGE gel obtained with deoxyribozyme construct EC3.

The activity of all deoxyribozymes, analyzed using synthetic DNA oligonucleotides containing an internal ^{32}P-labeled phosphodiester, was scored as described in Materials and Methods (see the first inset in Figure 1B). Generally speaking, a mutant deoxyribozyme with a score of +++++ or ++++ is regarded as an efficient catalyst (with estimated $k_{\text{obs}} \geq 0.01$ min^{-1}), while a sequence scored +++ or lower is treated as a poor catalyst. We also note that this scoring method was adopted simply to provide a convenient and experimentally manageable way to compare the relative activities of large number of mutant deoxyribozymes employed in this study.

Truncating Nucleotides in the Catalyst Domain. Progressive removal of nucleotides at the 3′ end of the catalyst domain was carried out first, and the data are presented in

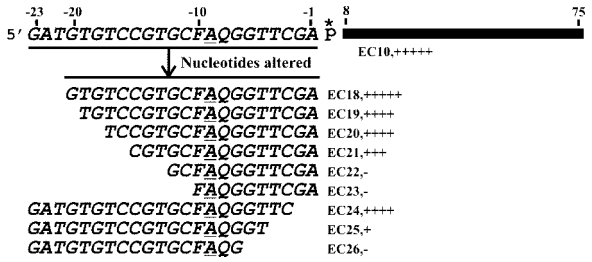

FIGURE 2: Nucleotide truncation in the substrate domain. The reference sequence is EC10. Underlined nucleotides are the region examined, with the vertical arrow pointing to all mutated sequences. The name of each mutant deoxyribozyme is listed next to each altered sequence. The activity of each deoxyribozyme construct is scored using the activity map shown in Figure 1B.

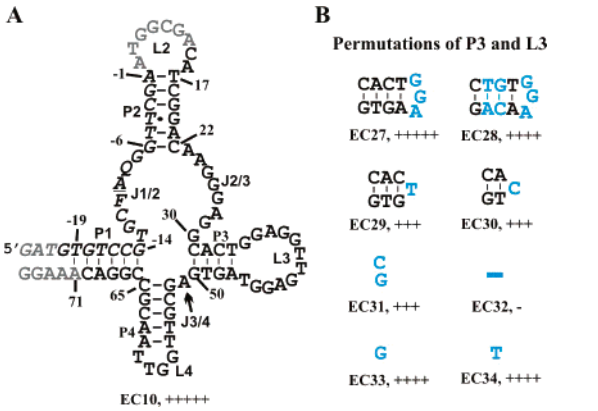

FIGURE 3: Proposed secondary structure of EC10 and role of nucleotides in P3 and L3. (A) The putative secondary structure of EC10, a truncated version of pH6DZ1. Individual elements are marked as P (pairing region), L (loop), and J (junction; single-stranded region between two pairing regions). Nucleotides in gray are dispensable nucleotides that can be removed without any loss of catalytic activity. Nucleotides in black are required for full activity up to the previous experiment (at least 10-fold activity reduction upon deletion or mutation). (B) Mutant deoxyribozymes with permutated P3 and/or L3 elements. The name of each mutant deoxyribozyme is given underneath each altered motif. The activity of each construct is scored using the activity map shown in Figure 1B. Nucleotides in blue are nucleotides altered in comparison to EC10. The thick short blue line denotes the deletion of the entire P3−L3 motif.

Figure 1B. Truncating as many as 30 nucleotides from the 3′ terminus had no apparent effect on the catalytic activity, as the mutant deoxyribozymes EC1−EC4 (E, enzyme; C, cis-acting) retained full catalytic activity. Removing one (EC5, +++) and two (EC6, ++) additional nucleotides from the same end resulted in a reduction in activity by 2 and 3 orders of magnitude, respectively. Further deletion of even one more nucleotide (EC7, -) completely abolished the RNA-cleaving activity. C_{70} and G_{68} are therefore the 3′-terminal nucleotides defining the fully active sequence and the minimally active sequence within the catalytic domain, respectively.

The effects of deleting nucleotides from the 5′ end of the catalyst domain were assessed next. The first 14 nucleotides in this region were completely dispensable, as the deletion of either 7 nucleotides (EC10, +++++) or 14 nucleotides (EC11, +++++) had no effect on the catalytic activity. Removing the next three nucleotides one at a time (EC12−14, all ++++) all caused about a 10-fold reduction in activity. Removing three (EC15, +++) and five (EC16, +) more nucleotides significantly reduced the catalytic activity, by approximately 100 and 10000-fold, respectively. When the deleted residues expanded to include A_{23} (EC17, -), the RNA-cleaving activity was completely eradicated. Therefore, C_{15} and A_{23} are the 5′-terminal nucleotides that define the fully active sequence and the minimally active sequence within the catalyst domain, respectively.

Truncating Nucleotides in the Substrate Domain. Several deoxyribozyme constructs with sequential nucleotide truncations from either the 5′ or 3′ end of the substrate domain were examined using EC10 as the reference deoxyribozyme; the data are provided in Figure 2. Removing the first three 5′-terminal nucleotides (EC18, +++++) had no effect on the catalytic activity. Constructs with one (EC19, ++++) and three (EC20, ++++) more nucleotides deleted from the same end both exhibited an activity ∼10-fold less than EC10. Another 10-fold reduction in activity was observed when two more nucleotides were removed from the substrate chain (EC21, +++). The RNA-cleaving activity was completely lost with the further removal of three (EC22, -) or five (EC23, -) nucleotides.

Interestingly, all nucleotides downstream of the cleavage site in the substrate domain were required for the optimal function of the deoxyribozymes, as deletion of even two nucleotides from the 3′ end of the substrate domain (EC24, ++++) lowered the catalytic activity by ∼10-fold. Removal of two more nucleotides from the same end (EC25, +) led to a new construct whose activity was weakened by ∼10 000-fold. Not surprisingly, the RNA cleavage activity was abolished upon deletion of two more nucleotides (EC26, -). These results indicate that a majority of nucleotides in the substrate domain are required for the catalytic function of the deoxyribozyme. It is possible that these nucleotides are engaged in extensive secondary or tertiary interactions that are responsible for substrate recognition.

A Putative Secondary Structure. Nucleotide truncation experiments not only established a significantly shortened cis-acting deoxyribozyme sequence but also implicated the functional involvement of up to 20 nucleotides in the original 23-nt substrate domain. Based on the fact that all known RNA-cleaving deoxyribozymes have used extensive Watson−Crick base-pairing interactions to engage substrate nucleotides both upstream and downstream of the cleavage site for binding (8−10, 14−16), we hypothesized that pH6DZ1 may adopt the same strategy for substrate recognition. Careful inspection of the sequence of the shortened deoxyribozyme EC10 indeed led to the identification of two short DNA duplexes, one on each end of the cleavage site (Figure 3A). The first duplex, denoted P1, is a 6-bp helix formed between G_{-14}−T_{-19} and C_{66}−A_{71}. The second one, deonoted P2, is also a 6-bp helix formed between A_{-1}−G_{-6} and T_{17}−C_{22}.

Searching the remainder of the sequence for additional Watson−Crick base pairs led to the discovery of two more putative short DNA duplexes named P3 and P4 (Figure 3A). P3 is a 4-bp helix formed between C_{31}−T_{34} and A_{47}−G_{50}, while P4 is a 6-bp helical region involving G_{52}−T_{56} and A_{61}−C_{65}. These four short duplexes create six single-stranded DNA elements referred to as L2 (L, loop; L2, the DNA loop attached to P2), L3, L4, J1/2 (J, junction; J1/2, the single-stranded sequence linking P1 and P2), J2/3, and J3/4 throughout this report. Most significantly, the multiple helical

and unstructured elements give pH6DZ1 a unique secondary structure that is different from those described for all known RNA-cleaving deoxyribozymes (*8*−*10*, *14*−*16*).

For the remaining figures in this report, the following nucleotide-coloring scheme will be used: nucleotides in gray can be safely removed without the loss of activity; nucleotides in black are required for full activity (mutating or deleting each of these nucleotides will result in a reduction in activity from +++++ to ++++), based on the results obtained from previous mutations; nucleotides in green are absolutely essential for catalysis (mutating any of these nucleotides will completely inactivate the deoxyribozyme); and nucleotides in red play an important, although nonessential, role in the catalytic function of the deoxyribozyme (mutating any of these nucleotides will result in a reduction in activity by at least 3 orders of magnitude, from +++++ to +++ or lower).

Permutations of P3 and L3. The first mutant deoxyribozyme in Figure 3B, EC27, was designed to test the dispensability of L3. In this deoxyribozyme construct, the original 12-nt L3 in the reference deoxyribozyme EC10 was replaced with an arbitrarily chosen GGA triloop. The fact that EC27 was fully active demonstrates that L3 has no relevance to the catalytic function of the deoxyribozyme. The next four deoxyribozymes, EC28−32, were designed to examine the importance of P1. In EC28, the two middle base pairs of P1 were altered from A−T and C−G to T−A and G−C, respectively. These changes resulted in moderate activity reductions (+++++ to ++++). The constructs in which the stem-loop element of EC10 was progressively reduced to 7 nt (EC29, +++), 5 nt (EC30, +++), and 2 nt (EC31, +++) all exhibited an RNA-cleaving activity that was reduced by 2 orders of magnitude, while the deletion of the entire P3-L3 motif (EC32, -) completely deactivated the deoxyribozyme. Interestingly, when a single nucleotide (G in EC33 and T in EC34) was inserted into the location of the deleted stem loop, most of the catalytic activity was recovered (++++). These results collectively demonstrate that P3 and L3 do not contain any catalytically essential or vital nucleotides. However, P3 appears to play a structural role that is important for the optimal activity of the deoxyribozyme.

Permutations of P4, L4, and J3/4. These three elements together cover the nucleotides from A_{51} to C_{65} (Figure 4). Alteration of base-pairing partners of each of the five base pairs in P4 resulted in a reduction in activity by 10−1000-fold, depending on the location of the specific base pair. Conversion of the first base pair (G_{52}−C_{65}) from G−C to C−G (EC35) or the second base pair (C_{53}−G_{64}) from C−G to G−C (EC36) caused only a 10-fold activity reduction. When the third base pair (G_{54}−C_{63}) was changed from G−C to A−T (EC38), no decrease in activity was observed; however, if the same base pair was altered to C−G pair (EC37), the activity dropped by 100-fold. Alteration of each of the last two base pairs (T_{55}−A_{62}, T_{56}−A_{61}) from T−A into any other base pair produced a much more profound change in the catalytic activity, as each mutant deoxyribozyme (EC39−43) was barely active.

Two mutant deoxyribozymes with a mismatch present at the second base pair (EC44, C−C mismatch) or third base pair (EC45, T−T mismatch) were also examined. With EC44, the catalytic activity was reduced by 100-fold, while

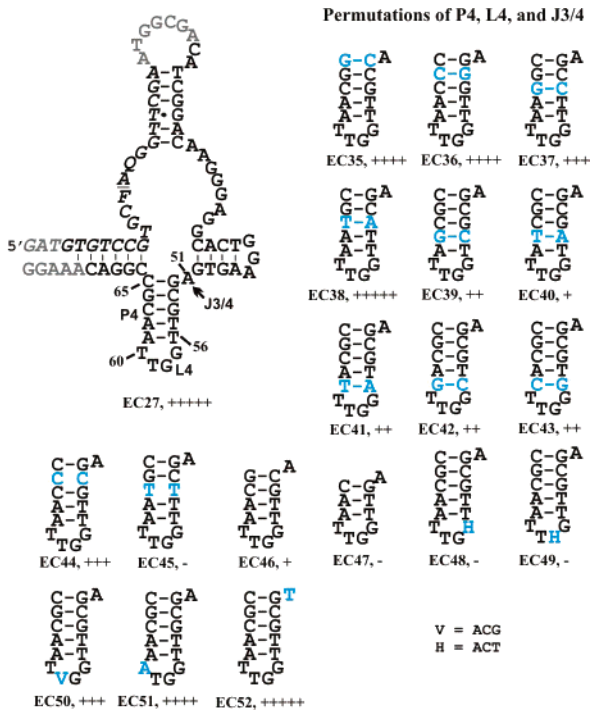

FIGURE 4: Permutations of P4, L4, and J3/4. The putative secondary structure of EC27 is shown on the left, and mutant deoxyribozymes with permutated P4 (EC35−47), L3 (EC48−51), or J3/4 (EC52) are shown on the right. The name of each mutant deoxyribozyme is given underneath each altered motif. Nucleotides shown in blue are the actual altered nucleotides in each construct in comparison to EC27. Other nucleotide coloring schemes are identical to those used in the previous figure. The activity scoring scheme is the same as that given in Figure 1B.

for EC45, the enzymatic activity was completely abolished. We also examined the influence of shortening P3 by eliminating one or two base pairs (EC46 and EC47, respectively). EC46 was catalytically very weak (EC46, +), while EC47 was completely inactive (EC47, -). Low activity (++) was also observed in the mutant deoxyribozyme in which an additional G−C pair was inserted above the two T−A pairs (data not shown). The above data can be interpreted as follows: (1) P3 does exist; (2) the identity of each base pair, particularly the last two base pairs, is important for the deoxyribozyme function; and (3) the size of P3 is also important for the function of the deoxyribozyme.

The 4-nt loop L4 was examined next. Changing G_{57} to T (data not shown) or H (equal mixture of ACT; EC48) resulted in no detectable activity. The same outcome was observed when G_{58} was changed to T (data not shown) or H (EC49). These experiments show that these two residues are absolutely required for catalytic function. In contrast, the last two nucleotides of L3, T_{59} and T_{60}, are not as essential because the mutant deoxyribozyme with the T-to-V mutation at nucleotide 59 (EC50; V, equal mixture of ACG) or the T-to-A mutation at nucleotide 60 (EC51) exhibited about $^1/_{100}$ and $^1/_{10}$ of the activity of the reference deoxyribozyme EC27, respectively.

Last, the identity of the single nucleotide, A_{51}, located between P3 and P4 was investigated. On the basis of the observation that no decrease in activity was produced when A_{51} was replaced with T_{52} (EC52), it can be concluded that this nucleotide is not a functionally vital residue.

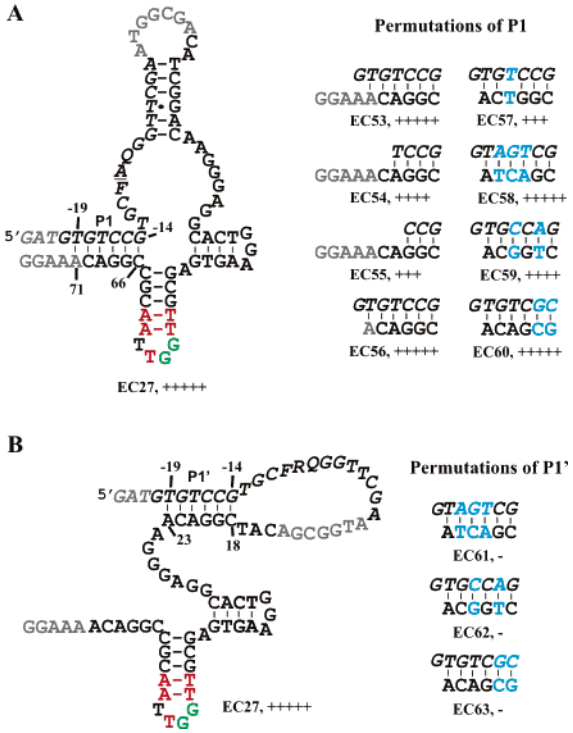

FIGURE 5: P1 and alternative P1 (P1′). (A) Deoxyribozyme constructs for examining the formation of P1. The putative secondary structure of EC27 is shown on the left, and the mutant deoxyribozymes within which P1 (formed between G_{-14}−T_{-19} and C_{66}−A_{71}) is permutated are shown on the right. (B) Alternative pairing between G_{-14}−T_{-19} and C_{18}−A_{23}. The name of each mutant deoxyribozyme is given underneath each altered motif. Nucleotides shown in blue are the actual altered nucleotides in each construct in comparison to EC27. Nucleotides in green are absolutely essential (no activity observed upon alteration); those in red are catalytically important (activity reduced by at least 100-fold after a base mutation). Other nucleotide coloring schemes are identical to those used in previous figures. The activity scoring scheme is same as that given in Figure 1B.

The above analyses led to the identification of two functionally essential nucleotides, G_{57} and G_{58} (colored green in Figure 5A), and five functionally important nucleotides in T_{55}, T_{56}, T_{59}, A_{61}, and A_{62} (labeled red in Figure 5A).

Permutations of P1. P1 is one of the two helices proposed to be responsible for substrate binding. Several deoxyribozyme constructs based on EC27 were designed to test whether P1 indeed exists and whether any nucleotide within P1 is critically involved in the catalytic function of the deoxyribozyme. The data are presented in Figure 5A.

Deletion of the first three overhanging nucleotides at the 5′ end of the substrate domain (G_{-23}−T_{-21}) had no influence on the catalytic activity (EC53, +++++). However, further removal of three and four additional nucleotides in the same domain, which resulted in a shortened P1 of only four and three base pairs, respectively, led to the deoxyribozyme constructs (EC54, ++++; EC55, +++) with activity weakened by 10- and 100-fold, respectively. Not surprisingly, most of the unpaired nucleotides at the 5′ end of the substrate domain and the 3′ end of the catalytic domain can be safely removed without any influence on the catalytic activity (EC56, +++++). However, deletion of G_{-4} resulted in a 10-fold activity reduction (data not shown). This finding, consistent with the data presented earlier (see EC19 in Figure 2), seems to suggest that G_{-4} may contribute to the stability of the relatively short duplex P1 or facilitate the geometric orientation of P1 in an optimally folded structure of the deoxyribozyme. The importance of a stable P1 was further manifested by the use of one additional construct, EC57: when a single mismatch pair was introduced in the middle of P1, the catalytic activity was reduced by 100-fold.

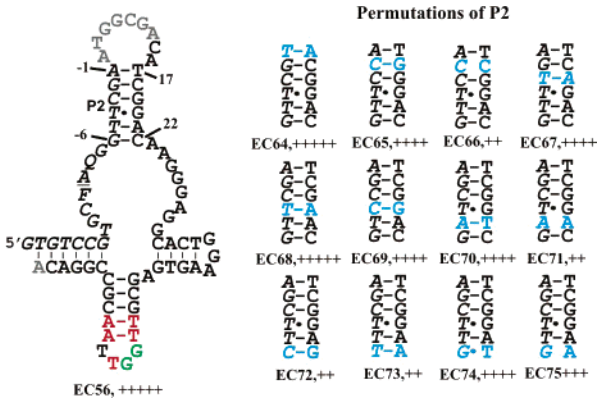

FIGURE 6: Permutations of P2. P2 is a 6-bp helix formed between A_{-1}−G_{-6} and T_{17}−A_{22}. The putative secondary structure of EC56 is shown on the left, and mutant deoxyribozymes within which P2 is permutated are shown on the right. The nucleotide coloring schemes and activity scoring methods are identical to those used in previous figures.

We next examined whether the identities of individual nucleotides within P1 were important for catalytic function by constructing three mutant deoxyribozymes, EC58−60, with significantly altered base pairs. EC58 has three consecutive central nucleotide covariations; EC59 has two separate internal covariations, while EC60 has two terminal covariations. All these mutant deoxyribozymes exhibited either full activity (EC58 and EC60, +++++) or near-full activity (EC59, ++++). The data given in Figure 5A allow us to conclude that (1) P1 does exist; (2) a stable P1 is required for the full activity of the deoxyribozyme; and (3) P1 does not contain any catalytically crucial nucleotide.

Alternative P1 (P1′). EC27 has an additional CGGACA motif located between the 18th and 24th nucleotides. This raises a possibility of alternative helical formation that involves G_{-14}−T_{-19} and C_{18}−T_{23}, and we term this alterative duplex P1′ (Figure 5B). Three new mutant deoxyribozymes, EC61−63, were designed to rule out the existence of P1′. EC61−63 were constructed with the same set of substrates used for EC58−60 but with corresponding changes in the C_{18}−A_{24} region (rather than C_{66}−A_{71} for EC58−60). None of these mutants exhibited any catalytic activity. This analysis convincingly demonstrates that G_{-14}−T_{-19} are pairing with C_{66}−A_{71} to form P1 and, therefore, not pairing with C_{18}−A_{23} to form P1′.

Permutations of P2. P2 is the second helical element for substrate recognition in the proposed secondary structure of pH6DZ1. To confirm the existence of this helical element and to probe the functional importance of individual nucleotides in this region, several mutant deoxyribozymes were examined. The data are shown in Figure 6.

When the A_{-1}−T_{17} pair was changed to the T−A pair, the full activity was maintained (EC64, +++++). When C_{-2}−G_{18} was switched to G−C (EC65, ++++), a 10-fold activity reduction was observed; however, the activity fell by 1000-fold when the same base pair was made into C−C mismatch (EC66, ++). When the C_{-3}−G_{19} pair was

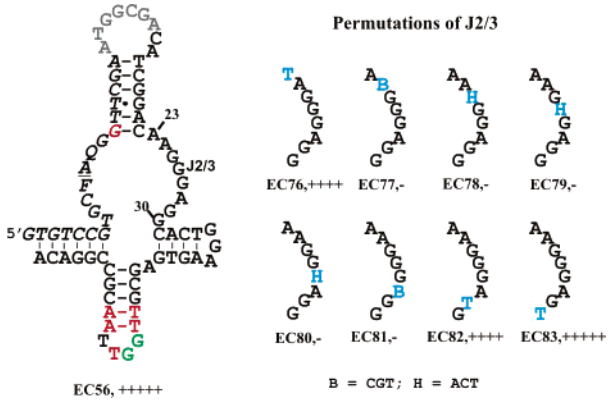

FIGURE 7: Permutations of J2/3. J2/3 is the single-stranded region covering the 23rd to 30th nucleotides. The putative secondary structure of the reference deoxyribozyme EC56 is shown on the left, and mutant deoxyribozymes each containing a single-base mutation within J2/3 are shown on the right. The nucleotide coloring scheme and activity scoring method are identical to those used in the previous figures.

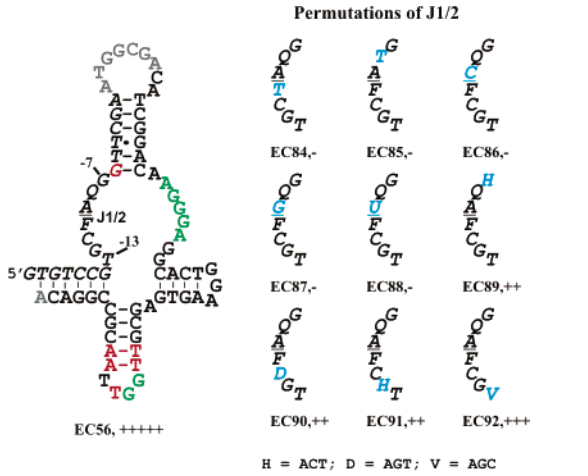

FIGURE 8: Permutations of J1/2. J1/2 is the single-stranded region located between the −7 and −13 nucleotides. The putative secondary structure of EC56 is shown on the left, and mutant deoxyribozymes containing a single-base mutation within J1/2 are shown on the right. The nucleotide coloring schemes and activity scoring methods are identical to those used in previous figures.

substituted with an A−T pair (EC67, ++++), the catalytic activity was reduced by 10-fold. When the T_{-4}•G_{20} wobble pair was mutated into a T−A pair (EC68, +++++), no reduction in activity was observed; if the same wobble pair was changed to the C−G pair (EC69, ++++), the activity decreased by 10-fold. When T_{-5}−A_{21} was switched to A−T, a 10-fold activity decrease was obtained; in contrast, replacing the same base pair with an A−A mismatch caused a 1000-fold reduction in activity. These data collectively suggest that the content of all these four base pairs was not very important to the function of the deoxyribozymes, as long as the Watson−Crick rules were followed.

The last base pair in P2, namely, the G_{-6}−C_{22} pair, behaved considerably differently. Changing G_{-6}−C_{22} either to C−G (EC72, ++) or to T−A (EC73, ++) led to a 1000-fold reduction in activity. In contrast, when G_{-6} was not mutated but C_{22} was changed to T (EC74, ++++) or A (EC75, +++), 10- and 100-fold reductions in activity were observed, respectively. These results could not conclusively support or rule out the formation of a proposed G_{-6}−C_{22} pair. However, it is certain that the identity of G_{-6} is vital for the enzymatic function.

Permutations of J2/3. J2/3 contains eight unpaired bases linking P2 and P3. Interestingly, all nucleotides in this motif are purine nucleotides. To examine the roles of these nucleotides, many mutant deoxyribozymes were synthesized and tested and the results are shown in Figure 7.

The mutant EC83 (+++++), containing a G-to-T mutation at the 30th nucleotide, exhibited full catalytic activity. The other two mutants, EC76 (++++) and EC82 (++++), which contained an A-to-T mutation at the 23rd position and a G-to-T mutation at the 29th position, respectively, showed relatively moderate (10-fold) reductions in activity. These findings indicate that none of these three purine nucleotides play critical roles in the function of the deoxyribozyme. Most importantly, the RNA-cleaving activity was completely lost in all the constructs in which A_{24}, G_{25}, G_{26} G_{27}, or A_{28} were mutated to T (data not shown) or to the mixture of the remaining nucleotides (B_{24}, H_{25}, H_{26}, H_{27}, B_{24}, respectively, in EC77, EC78, EC79, EC80, and EC81; B, equal mixture of CGT; H, equal mixture of ACT). These data reveal that these five nucleotides are essential to the catalytic function of the deoxyribozyme.

Permutations of J1/2. J1/2 is the single-stranded region that contains two specially modified deoxyribonucleotides Q_{-8} (DABCYL-dT) and F_{-10} (fluorescein-dT), the lone ribonucleotide $\underline{A}_{-9}$ (ribo-A), and four standard deoxyribonucleotides G_{-7}, C_{-11}, G_{-12}, and T_{-13} (Figure 8). Deoxyribozyme constructs in which either fluorescein (EC84), DABCYL (EC85), or both (data not shown) were removed exhibited no catalytic activity. This result indicates that both the fluorescein and DABCYL labels are crucial to the deoxyribozyme function.

The adenosine ribonucleotide is also a nucleotide specifically required for the deoxyribozyme function. This was revealed by the complete loss of activity in each of the three constructs in which the cleavage site was changed to either a cytidine ribonucleotide (EC86), a guanosine ribonucleotide (EC87), or a uridine ribonucleotide (EC88). This finding implies that the adenine attached to ribose is involved in highly specific interactions that are part of the active deoxyribozyme structure.

Three of the four remaining nucleotides within J1/2, G_{-7}, C_{-11}, and G_{-12}, appear to play crucial roles in the catalytic function of EC57 as well, because mutating any of these nucleotides to the mixture of the three remaining residues (G_{-7} to H_{-7}, EC89; C_{-11} to D_{-11}, EC90; G_{-12} to H_{-12}, EC91; H = ACT, D = AGT) weakened the RNA-cleaving activity by 1000-fold. The other nucleotide in this single-stranded region, T_{-13}, is only important for the optimal function of the deoxyribozyme as the T-to-V mutation (V = AGC, EC92) caused a 100-fold activity reduction.

DNA Footprinting via Methylation Interference. From the extensive mutagenesis studies presented above, it is clear that the active site of the deoxyribozyme must involve some or all of the 10 functionally essential nucleotides (green nucleotides in Figure 9A) located in J1/2, J3/4, and L4. Noticeably, half of these nucleotides contains a guanine base. Therefore, it is certain that some of these guanine residues are critically involved in the catalytic function of the deoxyribozyme.

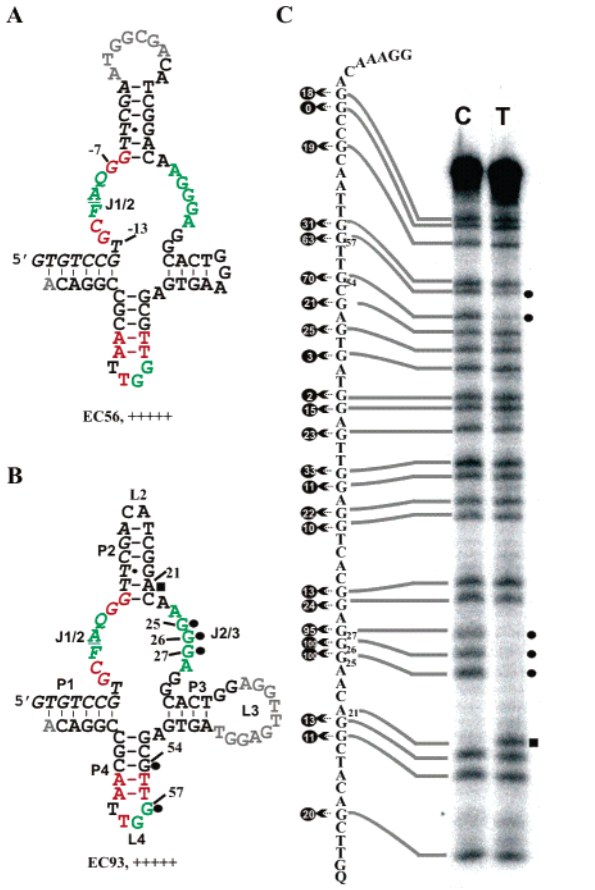

FIGURE 9: Methylation interference. (A) The confirmed secondary structure of fully functional deoxyribozyme EC56 with all nucleotides properly colored. (B) The secondary structure of fully functional deoxyribozyme construct EC93 with labeled nucleotides that have produced a methylation interference effect. The black circles indicate the guanines that have shown substantial methylation interference effect. The black square indicates the lone adenine that is significantly methylated. (C) Methylation data. 3′-Cleavage fragment obtained from EC93 treated with DMS before (test, T) or after (control, C) the cleavage reaction was performed and labeled at the 5′ end with ^{32}P. Under our reaction condition, DMS only methylated the N7 atom of one guanine per deoxyribozyme molecule. Methylated guanines were cleaved by piperidine, and cleaved fragments were resolved by denaturing 10% PAGE. Methylated guanines that disrupt deoxyribozyme activity appear lighter in lane T than lane C. The degree of interference at each guanine (each circled number) was normalized as described in Materials and Methods (with 0 being the minimal observable interference and 100 being the maximum). Filled black circles at the right side of the gel indicate the DNA bands with significantly reduced intensity (score of 50 and above) in T lanes, while the black square labels the DNA band that had a significantly enhanced intensity in the T lane.

We sought to use the methylation interference approach to obtain additional evidence that can further implicate these guanine residues in the tertiary folding or catalytic function of the deoxyribozyme. More specifically, we wanted to determine whether the methylation of the N7 atom of each functionally essential guanine within the fully functional deoxyribozyme construct EC57 (+++++) could be tolerated. Theoretically, the methylation of N7 of a functionally essential guanine residue is prohibited if any one of the following three scenarios applies: (1) the N7 atom is directly involved in a tertiary interaction that is essential for structural folding or catalytic function, (2) the N7 atom is located in a defined structural arrangement that cannot tolerate the bulky methyl group, and (3) the positive charge introduced by the methylation disrupts the vital electronic landscape where the guanine residue is located. In contrast, the guanine residues that have already been shown to be functionally insignificant usually should not produce a significant methylation interference effect.

For each methylation interference experiment, we used a set of two samples, which are denoted "control" and "test" (*13*). For the control sample, the methylation was performed on the 3′-cleavage product generated after the catalytic action of the cis-acting deoxyribozyme. When methylation is performed in water (where DNA exists in an unfolded random-coil state), every guanine residue should be methylated with approximately equal probability. Methylation was also carried out under a reaction condition that only allowed the methylation of one guanine per DNA molecule. Therefore, upon cleavage by piperidine and analysis by denaturing PAGE, DNA fragments, each corresponding to the cleavage product at a given guanine location, should be observed with relatively equal intensity. For the test sample, methylation with DMS in water was carried out with the deoxyribozyme construct prior to the self-cleavage reaction. If the methylation at a particular guanine residue hindered the self-cleaving activity of the deoxyribozyme, no RNA cleavage or significantly reduced RNA cleavage should occur in all individual DNA molecules that contained the methylated guanine. As a result, these molecules should be underrepresented in the cleaved product. This will eventually lead to a missing DNA band or a band with significantly reduced intensity on denaturing PAGE. In other words, methylated guanines that hindered proper enzymatic activity were identified by their absence or reduced visibility in the resultant ladder in the test lane (T lanes in Figure 9C) as compared to the control lane where all guanines are represented (C lanes in Figure 9C). The degree of interference was calculated using densitometry measurements of corresponding bands from each lane with a value of 100 indicating the most interference observed to 0 indicating the least. These values are given in the black circles shown next to their corresponding guanines within Figure 9C. Bases with values above 50 were considered to yield a substantial interference effect and were labeled with a filled circle next to the nucleotide within Figure 9B.

Among the five functionally essential guanines identified by mutagenic analysis, three (G_{25}, G_{26}, and G_{27}) exhibited extremely severe methylation interference and one (G_{57}) displayed a high level of interference. The only exception was G_{58}, which exhibited a less severe but still noticeable effect. The methylation of the N7 atom of a guanine located in standard duplexes and unstructured loops should not have a strong methylation interference effect. As expected, there is no substantial methylation interference for the guanines of P1, P2, P3, L3, and most guanines in P4. The only exception was G_{54}. Considering that G_{54} is located next to two functionally important T−A pairs and that the nearby L4 harbors two catalytically essential nucleotides, this finding is not very surprising. We suspect that L4 may interact with J1/2 and J2/3 to form the active site of the deoxyribozyme, and this may place G_{54} in a tight spatial arrangement that could not tolerate the methyl group on its N7 atom.

Interestingly, although most of the adenines within the deoxyribozyme were weakly methylated under our methy-

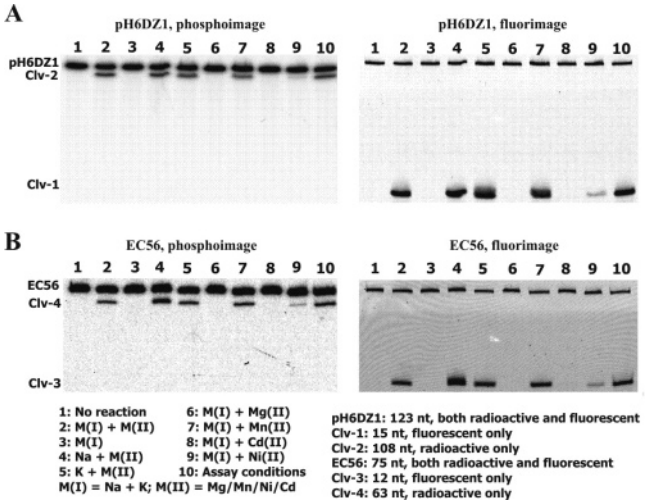

FIGURE 10: Comparison of metal-ion specificity of pH6DZ1 and EC56. Each DNA catalyst containing a ^{32}P-phosphodiester bond linking the substrate domain to the catalyst domain was tested for RNA cleavage under various salt conditions. The reaction products were analyzed on 10% denaturing PAGE, which was scanned for both radioactivity (left image) and fluorescence (right image). Clv-1 and Clv-2 denote the 5′ and 3′ cleavage products from pH6DZ1 and Clv-3 and Clv-4 are for the 5′ and 3′ cleavage products from EC56. Metal ions present are as follows (all in mM): no metal ions (lane 1); 400 Na^+, 100 K^+, 8.5 Mg^{2+}, 5 Mn^{2+}, 1.25 Cd^{2+}, and 0.25 Ni^{2+} (lane 2); 400 Na^+ and 100 K^+ (lane 3); 400 Na^+, 8.5 Mg^{2+}, 5 Mn^{2+}, 1.25 Cd^{2+}, and 0.25 Ni^{2+} (lane 4); 100 K^+, 8.5 Mg^{2+}, 5 Mn^{2+}, 1.25 Cd^{2+}, and 0.25 Ni^{2+} (lane 5); 400 Na^+, 100 K^+, and 15 Mg^{2+} (lane 6); 400 Na^+, 100 K^+, 10 Mg^{2+}, and 5 Mn^{2+} (lane 7); 400 Na^+, 100 K^+, 13.75 Mg^{2+}, and 1.25 Cd^{2+} (lane 8); 400 Na^+, 100 K^+, 14.75 Mg^{2+}, and 0.25 Ni^{2+} (lane 9); 800 mM Na^+, 8 mM Mn^{2+}, and 2 mM Ni^{2+} (lane 10; as the optimal metal ions established in ref *4*). Each reaction mixture also contained 50 mM MES, pH 6.0.

lation conditions (based on the observation that most of adenines were not cleaved after piperidine treatment), A_{21} was found to be hypermethylated. The precise reason for this finding cannot be determined at this point; however, we suspect that the observed hypermethylation may somehow relate to the fact that the G_{-6}−C_{22} pair adjacent to A_{21} did not tolerate any Watson−Crick covariation. It is possible that G_{-6} and C_{22} either do not engage themselves into a Watson−Crick base pair or form a highly unusual base pair that deviates significantly from the geometry of a standard Watson−Crick base pair. Methylation of the N7 of the nearby A_{21} may strongly stabilize the required geometric arrangement, and therefore, the methylated A_{21} was significantly over-represented in the cleaved product.

The above methylation interference experiment has provided strong evidence that further implicates the functional involvement of almost all of the indispensable guanine residues identified by mutational analysis.

Comparison of Metal-Ion Specificity and pH Dependence of pH6DZ1 and EC56. The original pH6DZ1 was known to function in the presence of both Mn(II) and Ni(II) but was incapable of performing catalysis in the presence of Mg(II) and Ca(II) (*4*). To determine whether the minimization of the catalytic DNA sequence altered the metal-ion specificity, an experiment was performed to compare the metal-utilizing abilities of the full-length pH6DZ1 and shortened EC56. The data are shown in Figure 10.

For this experiment, each deoxyribozyme was labeled with ^{32}P at the phosphodiester bond linking the substrate domain

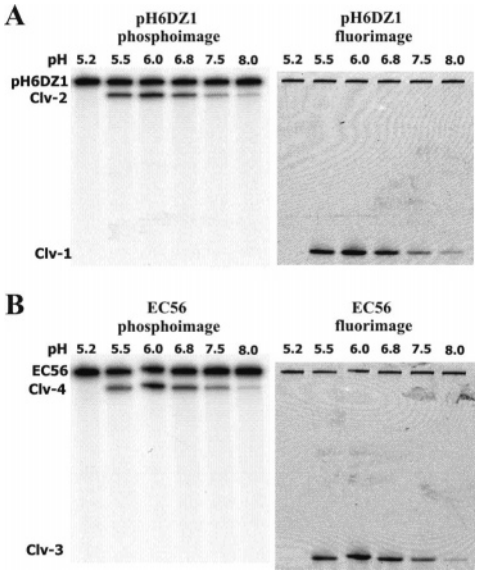

FIGURE 11: Comparison of pH dependence of pH6DZ1 and EC56. Each DNA catalyst containing a ^{32}P-phosphodiester bond linking the substrate domain to the catalyst domain was tested for RNA cleavage under various pH settings listed in the figure. The reaction products were analyzed on 10% denaturing PAGE, which was scanned for both radioactivity (left image) and fluorescence (right image). Clv-1 and Clv-2 denote the 5′ and 3′ cleavage products from pH6DZ1 and Clv-3 and Clv-4 are for the 5′ and 3′ cleavage products from EC56. Salt conditions were: 800 mM Na^+, 8 mM Mn^{2+}, and 2 mM Ni^{2+}. The solution pH was controlled with the following buffering reagents (each used at 50 mM): MES for pH 5.2 and 6.0; HEPES for pH 6.8, 7.5, and 8.0. These pH values were chosen according to ref *4*.

to the catalytic domain, in addition to having the standard fluorescein-dT, ribo-A, and DABCYL-dT moieties. This labeling pattern made the uncleaved deoxyribozyme (the top DNA bands in Figure 10, panels A and B, respectively) both fluorescent and radioactive. Upon RNA cleavage, two products were expected, a large DNA fragment (Clv-2 from pH6DZ1; Clv-4 from EC56; Figure 10) that was only radioactive and a small DNA fragment (Clv-1 from pH6DZ1; Clv-3 from EC56; Figure 10) that was only fluorescent. Moreover, for each reaction, the ratio of fluorescence intensity of the small cleavage fragment versus that of the uncleaved DNAzyme should be significantly larger than the ratio of radioactivity of the large fragment versus that of the uncleaved DNAzyme, because fluorescence dequenching was expected to occur upon cleavage.

When each deoxyribozyme was assessed for cleavage activity and scanned for both radioactivity (left image for each deoxyribozyme, Figure 10) and fluorescence (right image), the expected fragmentation and signaling patterns were indeed observed, indicating that each deoxyribozyme cleaved the embedded RNA linkage and produced a highly fluorescent 5′-cleavage fragment. More importantly, comparison of the cleavage bands clearly indicates that EC56 and pH6DZ1 have identical metal-ion specificity: both exhibited a strong activity with Mn^{2+} and a reduced activity with Ni^{2+}, but were incapable of using Mg^{2+} or Cd^{2+}.

We also conducted an experiment to compare the pH dependence of the same full-length and shortened DNAzymes, using the same procedure described above for the metal-ion specificity comparison. The data are presented in Figure 11. Not surprisingly, both pH6DZ1 and EC56 have identical pH

dependences: the highest activity occurs at pH 6.0; complete loss of activity is observed when the acidity of the solution increased to pH 5.2, and a progressive decrease in activity resulted when the solution pH was raised from pH 6.0 to 8.0.

The data illustrated in Figures 10 and 11 clearly indicate that the removal of the nonessential nucleotides from pH6DZ1 did not alter its metal-ion-binding properties or pH sensitivity of the original construct. Therefore, we can conclude that EC56 is a true representation of minimized pH6DZ1.

DISCUSSION

Through comprehensive sequence truncations, we have reduced the size of cis-acting pH6DZ1 from 123 nt to ~70 nt. Forty-four of these remaining nucleotides are distributed into four short helices of 4−6 base pairs each. All these helical nucleotides appear to play only structural roles that support the optimal activity of the deoxyribozyme, based on the observation that each of these nucleotides can tolerate a base mutation to some degree. Eighteen of the twenty-two base pairs can each be changed to another Watson−Crick base pair without significant loss of the catalytic activity. The three remaining base pairs, two in P4 and one in P2, are highly identity-specific, and replacing any of them with another Watson−Crick base pair can result in a loss of activity by 3 orders of magnitude. Interestingly, each of these three base pairs is located near a single-stranded region that contains some catalytically indispensable nucleotides. Therefore, these three base pairs may participate in some important interactions that support the formation of the active site.

Three hairpin loops also exist in the structure. Two of them, L2 and L3, do not appear to contain any functionally important nucleotide, and both loops can be significantly shortened without any reduction in activity. However, the remaining 4-nt loop L4 has two guanine residues that cannot be mutated. It is possible that these two guanines are part of the active site or at least participate in the tertiary interactions that are essential for the folding of the active deoxyribozyme structure.

The remaining 15 nucleotides are distributed into two interhelical single-stranded motifs, J1/2 and J2/3, of 7 and 8 nt, respectively. The 7-nt J1/2 possesses the ribonucleotide, the fluorophore-modified dT, and the quencher-modified dT, along with four other standard deoxyribonucleotides. The facts that neither the fluorophore nor the quencher can be removed and that the adenine located on the ribose at the cleavage site cannot be mutated into other bases, strongly suggest that these three moieties are essential for substrate recognition or contribute significantly to the formation of the active site. Three of the four remaining nucleotides in J1/2 were found to be functionally important, signifying that they may participate in important tertiary interactions that support the active site.

The 8-nt motif J2/3 contains five functionally essential nucleotides, all of which are purine bases. Considering that J2/3 is located in physical proximity to the cleavage-site-containing J1/2 and that most of the nucleotides in these two single-stranded regions are either indispensable or less prone to mutagenesis, we conclude that J2/3 and J1/2 must contribute the crucial nucleotides that form the active site of the deoxyribozymes.

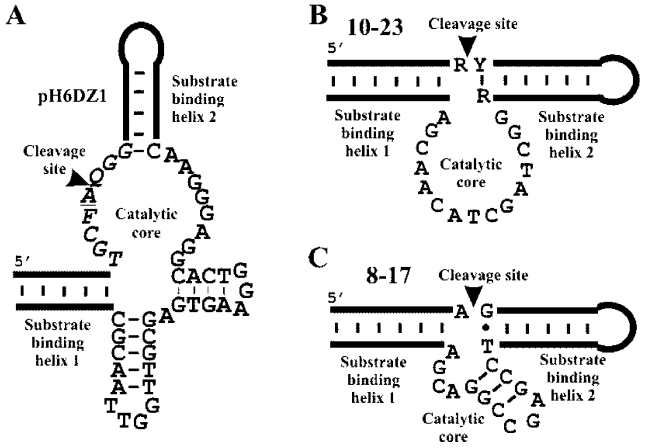

FIGURE 12: Comparison of the secondary structures of pH6DZ1 (A), 10-23 (B) and 8-17 (C). The substrate-binding duplexes in each deoxyribozyme are simplified through line drawing. Cleavage occurs at the position indicated by the arrow. R = A or G; Y = U or C.

Several RNA-cleaving deoxyribozymes that cleave a standard RNA substrate or an unmodified RNA/DNA chimeric substrate have been reported and characterized (*7*−*11*, *14*, *17*−*22*). All of these deoxyribozymes possess similar secondary structures. The elucidation of the secondary structure of pH6DZ1 allows us to make a comparison of the secondary structure features exhibited by pH6DZ1 with those seen with these RNA-cleaving deoxyribozymes. Figure 12 illustrates the secondary structures of the two most well-studied RNA-cleaving deoxyribozymes known as 10-23 and 8-17 (*9*, *17*) as the two representative RNA-cleaving deoxyribozymes, along with the secondary structure for EC56, a shortened but fully functional version of pH6DZ1.

The three deoxyribozymes share a common secondary-structure feature in that the substrate sequence is recognized by the catalytic domain through two short duplexes, one each upstream and downstream of the cleavage site. However, there are some noticeable differences between pH6DZ1 and the other two deoxyribozymes. First, the cleavage site of pH6DZ1 is located in the middle of several unpaired nucleotides, while that of both 10-23 and 8-17 is sandwiched immediately by the substrate-binding duplexes. This distinction may relate to the fact that pH6DZ1 has bulky fluorescein and DABCYL moieties placed on the two bases immediately surrounding the cleavage site, with both labels being absolutely required for the catalytic function. The participation of the bulky fluorescein and DABCYL groups in the tertiary folding may require that the nearby nucleotides adopt an unpaired configuration, resulting in a larger unpaired region near the cleavage site in pH6DZ1, as compared to that seen with 10-23 and 8-17.

Second, while 8-17 and 10-23 have a catalytic core of about 15 nucleotides, the shortened pH6DZ1 still uses more than 30 nucleotides to compose its catalytic core. The larger size of pH6DZ1 also results in the third difference: pH6DZ1 has a more complex secondary structure than the other two deoxyribozymes. The catalytic core of pH6DZ1 is comprised of two stem loops and one single-stranded region. By comparison, the catalytic core of 8-17 has one stem loop and a single-stranded region, while 10-23 has a catalytic core of 15 unpaired nucleotides. Interestingly, both pH6DZ1 and 8-17 distribute indispensable nucleotides into two single-

stranded regions that are separated by a short duplex. The rigidity of the duplex and the limited number of nucleotides in these single-stranded regions seem to suggest that it is difficult for these indispensable nucleotides to make direct contacts. Therefore, the precise functional roles of these essential but well-separated nucleotides remain to be deciphered. It is important to note that the catalytic core of each deoxyribozyme shares no apparent sequence conservation to any other DNAzyme, strongly indicating that each deoxyribozyme is a distinct class of RNA-cleaving deoxyribozyme.

The existence of multiple helical elements in the secondary structure of pH6DZ1 makes this unique deoxyribozyme versatile for the design of allosteric deoxyribozymes either by rational design using existing aptamers or by in vitro selection. This can be achieved using several principles established for the design and the in vitro selection of a large number of allosteric ribozymes and a few allosteric deoxyribozymes (*23*−*29*). With its synchronized catalysis−signaling capability, we expect that pH6DZ1 will find use in the design of fluorescence-signaling allosteric deoxyribozyme biosensors for the real-time detection of any chemical or biological target for which a DNA aptamer can be isolated. We are currently working on this front and will report our results in future publications.

REFERENCES

1. Joyce, G. F. (2004) Directed evolution of nucleic acid enzymes, *Annu. Rev. Biochem. 73*, 791−836.
2. Silverman, S. K. (2004) Deoxyribozymes: DNA catalysts for bioorganic chemistry, *Org. Biomol. Chem. 2*, 2701−2706.
3. Achenbach, J. C., Chiuman, W., Cruz, R. P., and Li, Y. (2004) DNAzymes: from creation in vitro to application in vivo, *Curr. Pharm. Biotechnol. 5*, 321−336.
4. Liu, Z., Mei, S. H., Brennan, J. D., and Li, Y. (2003) Assemblage of signaling DNA enzymes with intriguing metal-ion specificities and pH dependences, *J. Am. Chem. Soc. 125*, 7539−7545.
5. Mei, S. H., Liu, Z., Brennan, J. D., and Li, Y. (2003) An efficient RNA-cleaving DNA enzyme that synchronizes catalysis with fluorescence signaling, *J. Am. Chem. Soc. 125*, 412−420.
6. Li, J., and Lu, Y. (2000) A highly sensitive and selective catalytic DNA biosensor for lead ions, *J. Am. Chem.* Soc. *122*, 10466−10467.
7. Breaker, R. R., and Joyce, G. F. (1995) A DNA enzyme with Mg(2+)-dependent RNA phosphoesterase activity, *Chem. Biol. 2*, 655−660.
8. Breaker, R. R., and Joyce, G. F. (1994) A DNA enzyme that cleaves RNA, *Chem. Biol. 1*, 223−229.
9. Santoro, S. W., and Joyce, G. F. (1997) A general purpose RNA-cleaving DNA enzyme, *Proc. Natl. Acad. Sci. U.S.A. 94*, 4262−4266.
10. Feldman, A. R., and Sen, D. (2001) A new and efficient DNA enzyme for the sequence-specific cleavage of RNA, *J. Mol. Biol. 313*, 283−294.
11. Cruz, R. P., Withers, J. B., and Li, Y. (2004) Dinucleotide junction cleavage versatility of 8-17 deoxyribozyme, *Chem. Biol. 11*, 57−67.
12. Li, Y., and Breaker, R. R. (2001) In vitro selection of kinase and ligase deoxyribozymes, *Methods 23*, 179−190.
13. Achenbach, J. C., Jeffries, G. A., McManus, S. A., Billen, L. P., and Li, Y. (2005) Secondary-structure characterization of two proficient kinase deoxyribozymes, *Biochemistry. 44*, 3765−3774.
14. Roth, A., and Breaker, R. R. (1998) An amino acid as a cofactor for a catalytic polynucleotide, *Proc. Natl. Acad. Sci. U.S.A. 95*, 6027−6031.
15. Santoro, S. W., Joyce, G. F., Sakthivel, K., Gramatikova, S., and Barbas, C. F., III (2000) RNA cleavage by a DNA enzyme with extended chemical functionality, *J. Am. Chem. Soc. 122*, 2433−2439.
16. Lermer, L., Roupioz, Y., Ting, R., and Perrin, D. M. (2002) Toward an RNaseA mimic: a DNAzyme with imidazoles and cationic amines, *J. Am. Chem. Soc. 124*, 9960−9961.
17. Santoro, S. W., and Joyce, G. F. (1998) Mechanism and utility of an RNA-cleaving DNA enzyme, *Biochemistry. 37*, 13330−13342.
18. Schlosser, K., and Li, Y. (2004) Tracing sequence diversity change of RNA-cleaving deoxyribozymes under increasing selection pressure during in vitro selection, *Biochemistry. 43*, 9695−9707.
19. Li, J., Zheng, W., Kwon, A. H., and Lu, Y. (2000) In vitro selection and characterization of a highly efficient Zn(II)-dependent RNA-cleaving deoxyribozyme, *Nucleic Acids Res. 28*, 481−488.
20. Faulhammer, D., and Famulok, M. (1997) Characterization and divalent metal-ion dependence of in vitro selected deoxyribozymes which cleave DNA/RNA chimeric oligonucleotides, *J. Mol. Biol. 269*, 188−202.
21. Faulhammer, D., and Famulok, M. (1996) The Ca2+ ion as a cofactor for a novel RNA-cleaving deoxyribozyme., *Angew. Chem., Int. Ed. 35*, 2809−2813.
22. Peracchi, A. (2000) Preferential activation of the 8-17 deoxyribozyme by Ca(2+) ions. Evidence for the identity of 8-17 with the catalytic domain of the Mg5 deoxyribozyme, *J. Biol. Chem. 275*, 11693−11697.
23. Koizumi, M., Soukup, G. A., Kerr, J. N., and Breaker, R. R. (1999) Allosteric selection of ribozymes that respond to the second messengers cGMP and cAMP, *Nat. Struct. Biol. 6*, 1062−1071.
24. Roth, A., and Breaker, R. R. (2004) Selection in vitro of allosteric ribozymes, *Methods Mol. Biol. 252*, 145−164.
25. Soukup, G. A., and Breaker, R. R. (1999) Nucleic acid molecular switches, *Trends Biotechnol. 17*, 469−476.
26. Soukup, G. A., and Breaker, R. R. (1999) Engineering precision RNA molecular switches, *Proc. Natl. Acad. Sci. U.S.A. 96*, 3584−3589.
27. Soukup, G. A., and Breaker, R. R. (2000) Allosteric nucleic acid catalysts, *Curr. Opin. Struct. Biol. 10*, 318−325.
28. Levy, M., and Ellington, A. D. (2002) ATP-dependent allosteric DNA enzymes, *Chem. Biol. 9*, 417−426.
29. Robertson, M. P., and Ellington, A. D. (1999) In vitro selection of an allosteric ribozyme that transduces analytes to amplicons, *Nat. Biotechnol. 17*, 62−66.

BI050746F